CHINESE OPTICS LETTERS

Vol. 22, No. 3 | March 2024

Microstructured fluorescence in liquid crystals with femtosecond laser excitation

Xia Meng (孟 霞)[1], Ping Jin (金 萍)[1], Shijun Ge (葛士军)[2], Jiao Liu (刘 娇)[1], Bingxiang Li (李炳祥)[1*], Lei Wang (王 磊)[1,2,3**], and Yanqing Lu (陆延青)[2]

[1] College of Electronic and Optical Engineering & College of Flexible Electronics (Future Technology), Nanjing University of Posts and Telecommunications, Nanjing 210023, China

[2] National Laboratory of Solid State Microstructures, College of Engineering and Applied Sciences, Nanjing University, Nanjing 210093, China

[3] State Key Laboratory of Millimeter Waves, Southeast University, Nanjing 210096, China

*Corresponding author: bxli@njupt.edu.cn

**Corresponding author: wangl@njupt.edu.cn

Received September 30, 2023 | Accepted November 13, 2023 | Posted Online March 21, 2024

This study investigated direct fluorescence generation from a nematic liquid crystal (NLC) NJU-LDn-4 under femtosecond laser excitation. The absorption, transmittance, excitation, and emission spectra of the NLC were assessed. The relationship between the femtosecond pump power and fluorescence intensity was analyzed, revealing a quadratic increase and indicating that two-photon absorption (2PA) is the primary fluorescence mechanism. The LC microstructure was designed using photoalignment technology, allowing the generated fluorescence to reflect the corresponding structure. This research can establish a foundation for tunable LC microstructured fluorescence, with potential applications in fluorescence microscopy and optoelectronics.

Keywords: liquid crystal; femtosecond laser; fluorescence; microstructure.

DOI: 10.3788/COL202422.033801

1. Introduction

Liquid crystals (LCs) represent intermediate states between solids and liquids, exhibiting both crystal-like order and liquid fluidity. The distribution of the director and optical properties strongly depend on surface properties and temperature. LCs demonstrate high sensitivity to external fields and exhibit a broad range of dielectric anisotropies, allowing them to respond across a wide frequency range, from ultraviolet to microwave wavelengths[1]. Research in this field has been steadily advancing beyond information display applications and venturing into the exciting realm of photonics, demonstrating immense scientific potential[2].

LCs possessing fluorescence emission capabilities are referred to as luminescent LCs (LLCs). These materials exhibit LC properties with excellent luminescent characteristics[3], including linearly polarized emission[4] and circularly polarized luminescence[5], and are widely applied in fields such as optical information display[6]. LLCs can be created by doping them with fluorescent materials, such as fluorescent dyes[7], rare earth elements[8], and quantum dots[9]. Doping alters the optical properties of LCs, enabling them to emit fluorescent light. However, when fluorescent materials are introduced to form LLCs, they may interact with LC molecules, leading to fluorescence quenching, which reduces the fluorescence emission intensity. This limits the fluorescence performance of LCs and affects their applications. To address the issue of fluorescence quenching, in 2001, Tang *et al.* proposed aggregation-induced emission (AIE) in siloles[10]. LLCs can also be obtained by synthesizing LC-conjugated polymers, which offer advantages over previous approaches, including improved stability, a more uniform distribution of luminescent units[11], and facile processing[12]. Liu *et al.* constructed LLC molecules with efficient solid-state luminescence by chemically conjugating tetraphenylene cores with aggregation-induced luminescence and luminescent mesogenic tolane moieties[13]. Zhang *et al.* synthesized the first columnar rufigallol LC with AIE groups, demonstrating good fluorescence properties in an aggregated state[14]. The fluorescent properties of LLCs strongly depend on their molecular structure[15]. Yu *et al.* identified the fluorescence emission source as the biphenyl group in the polymer side chain, with the fluorescence intensity decreasing as the spacer length decreases[16]. Moreover, Tang *et al.* constructed fluorescence patterns based on LC copolymers using nanoimprint lithography[17]. Zhao *et al.* successfully achieved photopatterns in a luminescent LC device via photoalignment technology[18].

The process described earlier typically involves generating fluorescence in LCs via UV irradiation, resulting in down-conversion luminescence. In this process, the emitted wavelength is longer and has weaker photon energy than the input photon energy, following the principle of Stokes' rule. Another phenomenon, known as up-conversion luminescence, deviates from Stokes' rule and offers several advantages, including multicolor emission, strong penetration, a high signal-to-noise ratio, and multiphoton excitation[19]. Achieving up-conversion luminescence in LCs typically involves incorporating fluorescent materials via doping. For example, Guo *et al.* co-doped a chiral fluorescent photoswitch and up-conversion nanoparticles (UCNPs) into a nematic LC (NLC) medium to investigate the effects of up-conversion luminescence on reflective color switching and fluorescence tuning in cholesteric LC (CLC) cells[20].

Femtosecond-laser-induced materials generate two-photon absorption (2PA), resulting in up-conversion fluorescence. This advanced technology offers several advantages, such as high spatial selectivity, reduced photodamage, and enhanced sensitivity[21]. Therefore, studying the interaction between light and matter is crucial[22]. This process holds vast potential for applications in three-dimensional optical data storage[23] and two-photon-excited fluorescence microscopy[24]. Qian *et al.* measured the fluorescence spectra of 2PA and up-conversion fluorescence in symmetrical compounds using an 800-nm femtosecond laser. Furthermore, they studied the solvatochromic effect of these compounds in various solvents[25]. Vivas *et al.* examined the influence of aluminum content in $Al_xGa_{1-x}N$ thin films and the n-type doping concentration in GaN thin films on their 2PA coefficients by analyzing femtosecond-level 2PA spectra[26]. In their study on polycrystalline zinc selenide (ZnSe), excited by 775 nm, 1 kHz femtosecond laser pulses, Li *et al.* observed that the two-photon-induced fluorescence exhibited blue fluorescence and self-absorption near the band edge[27]. To date, femtosecond-laser-induced LCs generating up-conversion fluorescence and forming microstructured fluorescence have not been reported.

The introduction of fluorescent components into LCs and construction of LCP can complicate the pretreatment process, potentially limiting practical application of these materials. This study investigated the use of pure NLC material NJU-LDn-4 for direct fluorescence emission generated by a femtosecond laser, eliminating the need for additional fluorescent doping. Fluorescence was generated via the 2PA mechanism, and specific fluorescent microstructures were achieved using photoalignment technology. This approach enables the preparation of high-resolution luminescent two-dimensional patterns.

2. Experiment

The experimental setup for LC fluorescence generation using femtosecond laser excitation is shown in Fig. 1(a). The pump source used was a titanium sapphire femtosecond laser with a center wavelength of 800 nm, pulse width of 100 fs, and repetition rate of 1 kHz. The laser beam was incident parallel to the LC cell. Fluorescence spectra were measured using a spectrometer PG 2000 Pro. Meanwhile, a fluorescent beam with graphic information on the LC cell was monitored and recorded in real-time using a CCD camera, and the laser beam was loosely focused on the LC cell with a spot diameter of approximately 2 mm. The LC cell comprised two parallel fused silica substrates separated by 250-μm thick Mylar films and infiltrated with the LC NJU-LDn-4. Both substrates were spin-coated with a 0.5% (mass fraction) solution of sulfonic azo dye (SD1), which served as an alignment layer. The NJU-LDn-4 hybrid material mainly comprises derivatives with fluorinated biphenyltolanes[28], as illustrated in the inset. The presence of carbon–carbon triple bonds ensures a strong conjugation effect, and the biphenyl group is considered to be the main component of the fluorescence emission[16,29–31]. The experimental fluorescence of the sample is shown in Fig. 1(b).

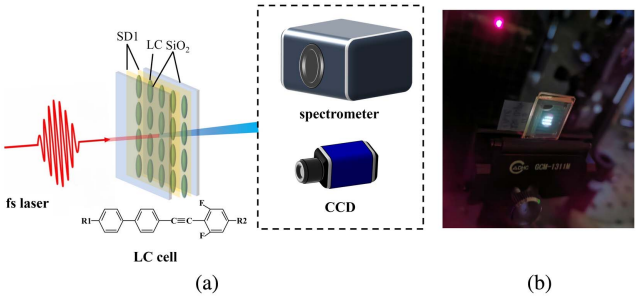

Fig. 1. (a) Schematic of the experimental setup for femtosecond laser-induced fluorescence up-conversion in LCs. The inset shows the primary components of NJU-LDn-4. (b) The experimental fluorescence of the sample.

3. Results and Discussion

3.1. Spectral measurement of the LC

The absorption and transmittance spectra of NJU-LDn-4 are shown in Figs. 2(a) and 2(b), respectively. The absorption intensity is highest at 400 nm, rapidly decreasing between 400 and 500 nm and then gradually slowing down beyond 500 nm. No absorption peak can be observed at 800 nm, and the absorption intensity is relatively low. The transmittance reaches its minimum at 400 nm and increases with increasing wavelengths. Figures 2(c) and 2(d) show the excitation and emission spectra, with central wavelengths of 390 nm and 450 nm, respectively, resulting in a Stokes shift of about 60 nm.

3.2. Comparison of the effects of femtosecond and continuous lasers on fluorescence

Continuous lasers with a wavelength of 405 nm were used to excite the LC and were compared to femtosecond laser excitation at 800 nm. A continuous purple laser was applied to the LC cell sample, and the detected spectrum is shown in Fig. 3(a). The LC exhibited fluorescence emission when excited by the purple laser with a central wavelength of 492 nm, resulting in

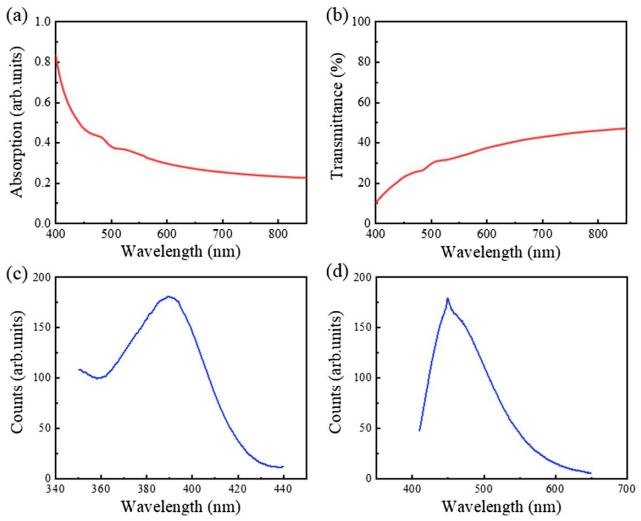

Fig. 2. (a) Absorption and (b) transmittance spectra of the NJU-LDn-4. (c) Excitation and (d) emission spectra of NJU-LDn-4.

blue fluorescence emission. The Stokes shift was 87 nm and a fluorescence image was captured under UV irradiation at 405 nm. The spectrum resulting from excitation of the LC using a femtosecond laser pulse is depicted in Fig. 3(b). Compared with UV-pumped single-photon fluorescence, it exhibits a similar fluorescence spectrum with a 9-nm shift in the central wavelength. The fluorescence image maintained its blue color. In contrast, employing a continuous laser operating at 808 nm to excite the LC resulted in the absence of fluorescence emission (not illustrated here). However, when stimulated by a femtosecond laser with a wavelength of 800 nm, the NJU-LDn-4 generated up-conversion fluorescence with a central wavelength of 501 nm. Consequently, a preliminary conclusion can be drawn: femtosecond laser excitation of NJU-LDn-4 involves two-photon absorption fluorescence.

The peak positions of the single- and two-photon fluorescence showed no significant changes, and strong fluorescence was visible to the naked eye. However, the obtained fluorescence image using the femtosecond laser exhibits a distinct concentric ring structure [inset of Fig. 3(b)]. Compared with the

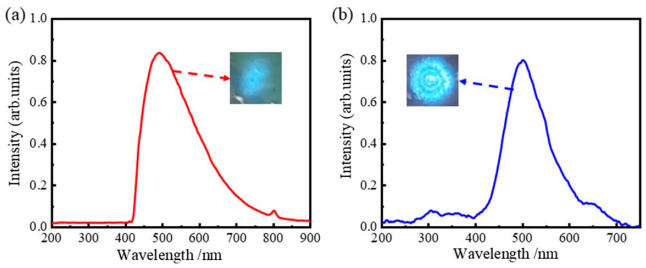

Fig. 3. (a) Fluorescence spectrum of the LC material excited by a 405-nm continuous laser. The inset shows the fluorescence generated by the continuous laser-induced LC cell. (b) Fluorescence spectrum of the LC material excited by an 800-nm femtosecond laser. The inset shows the fluorescence produced by the femtosecond laser-induced LC cell.

single-photon fluorescence generated by continuous laser excitation, the femtosecond laser confines the fluorescence to its focal point, and longer wavelengths are significantly less affected by scattering. Furthermore, two-photon fluorescence generated by the femtosecond laser offers a higher resolution. Under focused laser conditions, the 2PA effect can only be observed within a cubic region near the focal point corresponding to the excitation wavelength, whereas single-photon fluorescence occurs throughout the optical path.

3.3. Two-photon fluorescence characteristics

The fluorescence spectra of NJU-LDn-4 excited by the femtosecond laser at various pump powers are shown in Fig. 4(a). The fluorescence intensity increases gradually with power, experiencing a small enhancement from 0.5 to 1.5 W, followed by a significant enhancement from 1.5 to 3 W. When normalizing the fluorescence intensity at different pump powers, Fig. 4(b) illustrates the relationship between the fluorescence peaks and pump power, with experimental data indicated by black squares. The fluorescence intensity exhibits a clear quadratic growth trend, consistent with the theoretical relationship between the fluorescence intensity (I) and pump power (P) in up-conversion luminescence, as reported by Pollnau *et al.*[32],

$$I \propto P^n, \tag{1}$$

where I is the intensity of the up-conversion luminescence, P is the excitation power of the laser, and n is the number of photons absorbed by each photon emitted by the sample.

In this case, the relationship follows an equation with $n = 2$, indicating compliance with the principles of 2PA. The quadratic dependence of the fluorescence intensity on the pump power further confirms that the primary mechanism driving the fluorescence generation in the LC under femtosecond laser excitation is 2PA. We may also explore ultrafast phenomena related to femtosecond fluorescence up-conversion in LC in the near future.

3.4. Microstructured fluorescence

LC photoalignment technology is a non-contact method for aligning LCs using polarized light illumination. Unlike the

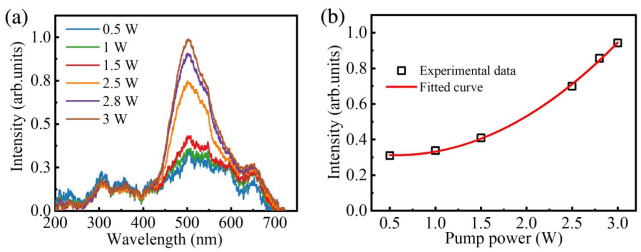

Fig. 4. (a) Fluorescence spectra of NJU-LDn-4 at different pump powers. (b) Quadratic fitting curve of fluorescence peaks under different pump power excitations.

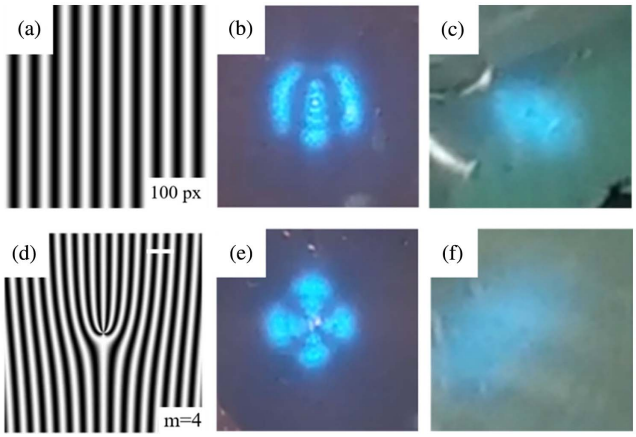

Fig. 5. (a) Periodic grating pattern (100 px represents one cycle) of the LC cell. (b) Fluorescence from the grating LC cell generated by a femtosecond laser and (c) continuous laser excitation. (d) Forked grating pattern with $m = 4$ and a scale bar of 100 μm. (e) Fluorescence of the forked LC cell generated by a femtosecond laser and (f) continuous laser excitation.

rubbing alignment method, this approach offers several advantages, including being pollution-free, electrostatic-free, and facilitating multidomain alignment in microregions[33]. The design involves using LC cells with microstructured patterns to investigate fluorescence emission phenomena and analyze fluorescence characteristics.

LC cell structures were designed using a digital micro-mirror device (DMD)-based dynamic microlithography system, which was utilized to perform a multi-step and partially overlapping exposure process to implement photopatterning on SD1, including a periodic grating structure, as shown in Fig. 5(a), along with a corresponding computer-generated hologram[34] featuring a topological charge value of $m = 4$, as depicted in Fig. 5(d).

The fluorescence of the LC cells under femtosecond laser and continuous laser induction was investigated. Figures 5(b) and 5(e) show clear fluorescence striped and quadruple patterns generated by the femtosecond laser. Figures 5(c) and 5(f) show the fluorescence under continuous laser UV excitation, with no observable patterns. The microstructure design in the LC cell of the NJU-LDn-4 material directly influenced the fluorescence patterns generated by the femtosecond laser. We believe that under the femtosecond laser excitation, the LC initially produces fluorescence, which is then modulated by the microstructure of the LC, resulting in the observed patterns. Compared with continuous laser induction, femtosecond lasers produce two-photon fluorescence using longer wavelengths, resulting in less damage and deeper penetration. Consequently, the generated fluorescence patterns were clearer. Based on these properties, all types of fluorescence patterns can be generated by designing the LC microstructures.

4. Conclusion

This study presents the phenomenon of fluorescence generated by a femtosecond laser in NLCs. The fluorescence, absorption, and transmission spectra of NJU-LDn-4 were analyzed and compared with single-photon fluorescence generated by continuous laser excitation. The physical mechanism of femtosecond-laser-induced LC fluorescence emission was determined to be 2PA. Photoalignment of LC microstructures produces high-resolution fluorescence patterns under femtosecond laser irradiation, in contrast to continuous UV laser irradiation. Because LCs are excellent electro-optic materials, their fluorescence can be dynamically adjusted by applying voltage. These findings can advance the development of functional fluorescent LCs, especially in creating tunable fluorescence patterns via photoalignment technology. Such advancements may find applications in fluorescence microscopy imaging, advanced optoelectronic devices, optical information processing, and biochemical sensing.

Acknowledgements

This work was supported by the National Key Research and Development Program of China (No. 2022YFA1405000), the Natural Science Foundation of Jiangsu Province (Nos. BK20211277 and BK20210179), the National Natural Science Foundation of China (NSFC) (No. 62105143), the Frontier Leading Technology Basic Research Project of Jiangsu Province (No. BK20212004), and the Postgraduate Research & Practice Innovation Program of Jiangsu Province (No. KYCX23_0971).

References

1. H. Maune, M. Jost, R. Reese, *et al.*, "Microwave liquid crystal technology," Crystals **8**, 355 (2018).
2. Y.-Q. Lu and Y. Li, "Planar liquid crystal polarization optics for near-eye displays," Light Sci. Appl. **10**, 122 (2021).
3. M. P. Aldred, A. J. Eastwood, S. M. Kelly, *et al.*, "Light-emitting fluorene photoreactive liquid crystals for organic electroluminescence," Chem. Mater. **16**, 4928 (2004).
4. Y. Wang, J. Shi, J. Chen, *et al.*, "Recent progress in luminescent liquid crystal materials: design, properties and application for linearly polarised emission," J. Mater. Chem. C **3**, 7993 (2015).
5. S. Lin, Y. Tang, W. Kang, *et al.*, "Photo-triggered full-color circularly polarized luminescence based on photonic capsules for multilevel information encryption," Nat. Commun. **14**, 3005 (2023).
6. Y. Sagara and T. Kato, "Brightly tricolored mechanochromic luminescence from a single-luminophore liquid crystal: reversible writing and erasing of images," Angew. Chem. Int. Ed. Engl. **123**, 9294 (2011).
7. J.-M. Choi, T.-Z. Shen, J. K. Vij, *et al.*, "Thermochromic luminescence in dual-dye-doped liquid crystal mixture induced by varying the energy transfer rate," Dyes Pigm. **180**, 108450 (2020).
8. R. Van Deun, D. Moors, B. De Fré, *et al.*, "Near-infrared photoluminescence of lanthanide-doped liquid crystals," J. Mater. Chem. **13**, 1520 (2003).
9. M. Bugakov, S. Abdullaeva, P. Samokhvalov, *et al.*, "Hybrid fluorescent liquid crystalline composites: directed assembly of quantum dots in liquid crystalline block copolymer matrices," RSC Adv. **10**, 15264 (2020).
10. J. Luo, Z. Xie, J. W. Y. Lam, *et al.*, "Aggregation-induced emission of 1-methyl-1,2,3,4,5-pentaphenylsilole," Chem. Commun. **381**, 1740 (2001).
11. O. Younis, M. Abdel-Hakim, M. M. Sayed, *et al.*, "Liquid crystal polymers as luminescent coatings: single-component white-light photoluminescence and corrosion inhibition," J. Lumin. **239**, 118361 (2021).
12. Y. Deng, M. Wang, Y. Zhuang, *et al.*, "Circularly polarized luminescence from organic micro-/nano-structures," Light Sci. Appl. **10**, 76 (2021).
13. Y. Liu, L. H. You, F. X. Lin, *et al.*, "Highly efficient luminescent liquid crystal with aggregation-induced energy transfer," ACS Appl. Mater. Interfaces **11**, 3516 (2019).

14. X. Zhang, W. Qin, B. Cheng, *et al.*, "First columnar rufigallol liquid crystals with high fluorescence at aggregated states," J. Mol. Liq. **298**, 112074 (2020).
15. H. W. Huang, K. Horie, T. Yamashita, *et al.*, "Fluorescence study on intermolecular interactions between mesogenic biphenyl moieties of a thermotropic liquid-crystalline polyester (PB-10)," Macromolecules **29**, 3485 (1996).
16. Z.-Q. Yu, X. Zhang, Z.-C. Li, *et al.*, "Fluorescence behavior of biphenyl containing side-chain liquid crystalline polyacetylene with various lengths of spacers," Acta Phys. Chim. Sin. **26**, 2281 (2010).
17. J.-C. Zhu, T. Han, Y. Guo, *et al.*, "Design and synthesis of luminescent liquid crystalline polymers with "jacketing" effect and luminescent patterning applications," Macromolecules **52**, 3668 (2019).
18. D. Zhao, F. Fan, V. G. Chigrinov, *et al.*, "Aggregate-induced emission in light-emitting liquid crystal display technology," J. Soc. Inf. Disp. **23**, 218 (2015).
19. F. Auzel, "Upconversion and anti-Stokes processes with f and d ions in solids," Chem. Rev. **104**, 139 (2004).
20. A. Juan, S. Lin, Y. He, *et al.*, "Near-infrared light-induced photoisomerization and photodissociation of a chiral fluorescent photoswitch in cholesteric liquid crystals assisted by upconversion nanoparticles," Soft Matter **17**, 1404 (2020).
21. O. V. Przhonska, S. Webster, L. A. Padilha, *et al.*, "Two-photon absorption in near-IR conjugated molecules: design strategy and structure–property relations," in *Advanced Fluorescence Reporters in Chemistry and Biology I* (Springer, 2010), p. 105.
22. G. H. Oliveira, F. S. Ferreira, G. F. Ferbonink, *et al.*, "Femtosecond laser induced luminescence in hierarchically structured Nd^{III}, Yb^{III}, Er^{III} co-doped upconversion nanoparticles: light-matter interaction mechanisms from experiments and simulations," J. Lumin. **234**, 117953 (2021).
23. D. A. Parthenopoulos and P. M. Rentzepis, "Three-dimensional optical storage memory," Science **245**, 843 (1989).
24. M. A. Albota, C. Xu, and W. W. Webb, "Two-photon fluorescence excitation cross sections of biomolecular probes from 690 to 960 nm," Appl. Opt. **37**, 7352 (1998).
25. Y. Qian, X. Q. Zhu, W. Huang, *et al.*, "Two-photon absorption and upconversion fluorescence by using a femtosecond Ti:sapphire laser in symmetrical chromophores," J. Funct. Mater. **39**, 1774 (2008).
26. M. G. Vivas, D. S. Manoel, J. Dipold, *et al.*, "Femtosecond-laser induced two-photon absorption of GaN and $Al_xGa_{1-x}N$ thin films: tuning the nonlinear optical response by alloying and doping," J. Alloys Compd. **825**, 153828 (2020).
27. Q. Li, W. Perrie, Z. Li, *et al.*, "Two-photon absorption and stimulated emission in poly-crystalline zinc selenide with femtosecond laser excitation," Opto-Electron. Adv. **5**, 210036 (2022).
28. L. Wang, X.-W. Lin, X. Liang, *et al.*, "Large birefringence liquid crystal material in terahertz range," Opt. Mater. Express **2**, 1314 (2012).
29. E. C. Lim and Y. H. Li, "Luminescence of biphenyl and geometry of the molecule in excited electronic states," J. Chem. Phys. **52**, 6416 (1970).
30. D.-E. Wu, Q.-Y. Yin, and Q.-H. Guo, "Position of biphenyl group turning the structure and photophysical property of D-π-π-A prototype fluorescent material," J. Fluoresc. **32**, 1369 (2022).
31. Y. M. Huang, J. W. Y. Lam, K. K. L. Cheuk, *et al.*, "Strong luminescence from poly(1-alkynes)," Macromolecules **32**, 5976 (1999).
32. M. Pollnau, D. R. Gamelin, S. R. Lüthi, *et al.*, "Power dependence of upconversion luminescence in lanthanide and transition-metal-ion systems," Phys. Rev. B **61**, 3337 (2000).
33. V. G. Chigrinov, V. M. Kozenkov, and H.-S. Kwok, *Photoalignment of Liquid Crystalline Materials: Physics and Applications* (Wiley, 2008).
34. A. V. Carpentier, H. Michinel, J. R. Salgueiro, *et al.*, "Making optical vortices with computer-generated holograms," Am. J. Phys. **76**, 916 (2008).